Flame Spread Behavior of Char-Forming Wall/Ceiling Insulating Materials

JEFFREY S. NEWMAN and ARCHIBALD TEWARSON
Factory Mutual Research Corporation
1151 Boston–Providence Turnpike
Norwood, Massachusetts 02062, USA

ABSTRACT

The extent of fire propagation and upward spread velocity are examined for char-forming insulating materials. The extent of propagation can be defined by the critical heat flux boundary, while reduced-scale propagation experiments are shown to represent accurately large scale corner fire behavior. In wall/ceiling applications, inert facings are shown to significantly limit the extent of fire propagation even for materials exhibiting self-sustained propagation. The "apparent" flame spread velocity for these types of char-forming materials correlates well with the ratio of the convective heat release rate to the surface thermal response.

KEYWORDS: Flame spread, heat transfer, material properties, char-forming materials.

INTRODUCTION

Char-forming materials enhance fire safety through carbon retention in the solid phase, resulting in reduced heat transfer and vapor generation (especially soot and other carbon containing compounds), and enhanced ignition and fire spread resistance. For char-forming materials, the fire spread behavior is very different from that of noncharring materials. Upon ignition, typically a rapid spread across the surface occurs, which is followed by immediate surface charring. The flames occasionally remain attached, but more often recess rapidly towards the ignition zone. Usually, only about 10 to 15% of the material mass is consumed in this process. In typical applications (e.g., building wall/ceiling insulation panels), an inert metal facing, ranging from 0.02 mm aluminum foil to 0.5 mm sheet steel, is installed on the material surface which prevents the rapid spread. There is, however, flame spread in the ignition zone due to delamination of the metal facing, with the extent of ultimate fire propagation beyond the ignition region the main concern. This paper attempts to investigate, in this general application, the importance of various material characteristics and couple them with results from both small-scale flame spread and large-scale 7.6 m (25 ft) Corner Tests.

CONCEPTS

Several relationships have been postulated within this paper, which are later shown to be supported by experimental evidence. These relationships,

which may be termed concepts, are "global" in nature and characterize the fire properties of insulating materials as well as the exposure fire environment contributing to fire propagation.

Ignition and Thermal Response

The critical heat flux ($\dot{q}''_{cr}$) is perhaps the useful ignition characteristic for materials. $\dot{q}''_{cr}$, the heat flux at or below which ignition is not expected to occur, is obtained by plotting the inverse of the time to piloted ignition, ($1/t_{ig}$) versus the applied external flux ($\dot{q}''_e$) as well as by performing experiments at the external value close to the critical heat flux. The critical flux is defined as the value of $\dot{q}''_e$ at which $1/t_{ig}$ is zero.

The surface temperature at ignition (T_{ig}) at or below which ignition cannot be achieved can be estimated from $\dot{q}''_{cr}$ using the following equation:

$$T_{ig} = (\alpha \dot{q}''_{cr}/\sigma)^{\frac{1}{4}} \qquad (1)$$

where α is the surface absorptivity (typically assumed to be unity for "black" surfaces) and σ is the Stefan-Boltzmann constant. In addition, when a thermally thick material is subjected to an external heat flux, the initial surface temperature history can often be approximated by the following transient heat conduction equation for linear heat flow in a semi-infinite solid:

$$\Delta T_{ig} = 2 \dot{q}''_e (t_{ig}/\pi k\rho c)^{\frac{1}{2}} \qquad . \qquad (2)$$

The thermal response parameter (TRP) [1] is defined as $\Delta T_{ig}(\pi k\rho c)^{\frac{1}{2}}/2$, which is obtained from the inverse of the slope of $t_{ig}^{-1/2}$ plotted against $\dot{q}''_e$).

Heat Release Rate

The "chemical" heat generation rate ($\dot{Q}''_{ch}$) of a material in a fire is the heat release rate from chemical reactions where carbon dioxide (CO_2) and carbon monoxide (CO) are the main products, and combustible vapors and oxygen are the main reactants, and is determined experimentally from the generation rates of CO_2 and CO. For a given material, $\dot{Q}''_{ch}$ is a function of the chemical heat of combustion (ΔH_{ch}), the heat of gasification for the material (L) and the net heat flux received by the material, i.e.,

$$\dot{Q}''_{ch} = (\Delta H_{ch}/L) (\dot{q}''_e + \dot{q}''_f - \dot{q}''_{rr}) \qquad (3)$$

where $\dot{q}''_e$, $\dot{q}''_f$ and $\dot{q}''_{rr}$ are the externally supplied heat flux, the flame heat flux, and the surface reradiative loss, respectively. Unfortunately for charring insulating materials, L is not constant. Therefore, an "effective" heat of gasification (L_e) needs to be used in Eq. (3). The exact method for obtaining values of L_e for the various materials studied is described in detail in the results.

Thermal Environment

The thermal environment in large fires is dominated by the radiative heat transfer from hot fire products. The net radiative heat flux received by a surface can be given by an expression similar to Eq. (1):

$$\dot{q}''_r = F_{sr} \sigma (\alpha T_r^4 - \varepsilon T_s^4) \qquad (4)$$

where $\dot{q}_r''$ is the heat flux; F_{sr} is the view factor (less than or equal to one) between the surface and the hot fire products; α and ε are the surface absorptivity and emissivity, respectively; and T_r and T_s are the temperatures of the radiation source and surface, respectively. For gray surfaces, α is independent of the spectral-energy distribution of the incident radiation and ε can be substituted for α into Eq. (4). If the thermal environment is optically thick, then F_{sr} becomes one and T_r can be approximated by the local gas temperature T_g.

Experiments

In this study, flame spread on char-forming wall/ceiling insulation materials was examined using vertical sheets 0.61 m, 4.9 m, and 7.6 m in length, where the 7.6 m sheets were installed as typical building interior finish wall/ceiling panels in a corner configuration. Fire propagation behavior was examined for the: 1) extent of propagation ; 2) characteristic heat release rate; and 3) maximum "apparent" flame velocity versus height.

Four sets of experiments were performed using six polyurethane and isocyanurate insulations and one "reference" polyester/fiberglass material. Tests were performed in our 50 kW-, 500 kW- and 10,000 kW-Scale Flammability Apparatuses (described in detail elsewhere [1], as well as in the 7.6-m (25-ft) Corner [2,3].

For each material, the 50 kW-Scale Apparatus was used to determine the following properties: 1) the critical heat flux; 2) the thermal response parameter; 3) the heats of combustion (chemical and convective); and 4) the "effective" heat of gasification. The critical flux was determined from the ignition experiments for 0.1 m square samples (surface coated with lamp black). The samples were exposed to known radiant heat flux values, and time to ignition was measured. The chemical and convective heats of combustion and the effective heat of gasification were determined by measuring the sample mass loss rate, generation rates of CO and CO_2, total mass flow rate of fire product-air mixture and sensible heat during exposure to an external heat flux of 50 kW/m^2.

In the 500 kW-Scale Apparatus, 51 by 102 mm by 610 mm long samples were used in a vertical orientation. Each sample was surrounded by a Pyrex tube 300 mm diameter and 610 mm in length extended to 1.2 m by a thin-walled stainless steel tube. Oxygen was introduced in the gas flow to enhance radiative flame heat transfer [4] at the bottom of the apparatus to produce a 40% concentration with a gas velocity of 0.11 m/s. The sample was surrounded by four coaxially placed tungsten-quartz radiant heaters. A small pilot flame about 1 mm in length located about 1 mm from the base of the sample surface provided the ignition source. All the products generated during flame propagation were collected in a sampling duct with measurements made similar to those in the 50 kW-Scale Apparatus. Figure 1 shows the 50 kW/m^2 peak external heat flux profile as a function of height (h) at the sample surface.

In the 10,000 kW-Scale Apparatus, two 4.9 m long by 0.61 m wide vertical panels separated by 0.30 m were used. A 61 kW propane sand burner (with an average flame height of approximately 0.6 m) was placed at the base between the two panels. Measurements similar to those in the 50 and 500 kW-Scale Apparatuses were made during fire propagation.

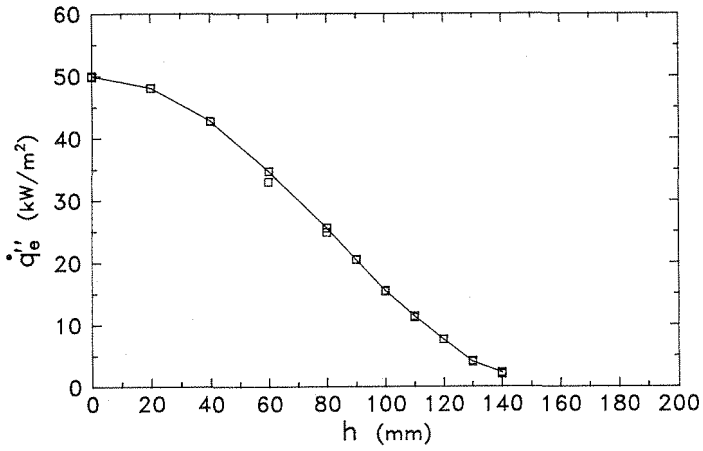

FIGURE 1. External heat flux versus height in the 500 kW-scale apparatus.

For the experiments conducted in the 7.6-m Corner, the samples were installed in a panel configuration (consisting of a metal skin over the insulating core material) on both the walls and ceiling (Fig. 2).

The material was subjected to a growing exposure fire (peak heat release rate of about 3 MW) comprised of approximately 340 kg wood pallets (1.2-m by 1.2-m) stacked 1.5-m high at the base of the corner. The extent of fire propagation was determined both visually at the end of each experiment (15 min in duration) and by the critical heat flux boundary. For determining the critical heat flux boundaries, heat fluxes (convective plus radiative) and gas temperatures were measured at the locations identified in Fig. 2. The figure is an isometric representation of the corner configuration with the dotted lines spaced a constant 2.5 m apart, i.e., H/3 separation where H is the ceiling height (7.6 m). The numbers in Fig. 2 are peak heat fluxes determined in blank experiments where only gypsum wallboard on the walls and ceiling was used. Based on the correlation between measured temperature and heat flux, which was found to follow radiative heat transfer relationships

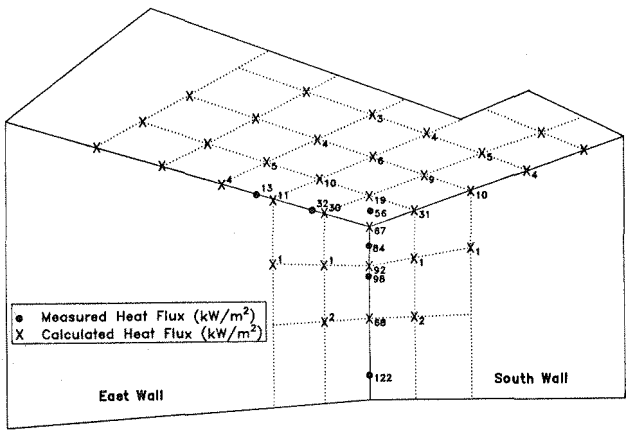

FIGURE 2. Heat flux calibration data for the 7.6-m Corner.

[2,3], the heat fluxes at other locations were inferred from the local gas temperatures using Eq (4).

RESULTS

Flame spread and associated data obtained in this study are listed in Table 1.

TABLE I. FLAME SPREAD AND ASSOCIATED DATA

Sample No.	1[a]	2[a]	3[a]	4[b]	5[b]	6[c]	7[d]
ρ (kg/m^3)	35	37	32	32	34	34	1670
ΔH_t (kJ/g)	23.2	21.5	28.7	24.4	22.9	22.6	14.2
χ_{ch}	0.59	0.47	0.53	0.51	0.59	0.71	0.61
χ_c	0.09	0.10	0.12	0.19	0.09	0.26	0.42
χ_r	0.50	0.37	0.41	0.32	0.50	0.45	0.19
L_e (kJ/g)	3.4	1.3	5.3	3.7	3.2	6.4	2.3
$\dot{q}''_{cr}$ (kW/m^2)	20	14	17	27	37	14	13
TRP (kW/m^{2}s$^{-1/2}$)	64	63	97	79	55	76	700
v_{max} (mm/s)	105	179	90	115	69	129	-
h_{max} (mm)	370	609	287	390	256	445	105
t_p (m)	6.86	9.45	6.55	7.32	6.25	8.53	5.64

[a] Polyurethane
[b] Isocyanurate
[c] Modified Isocyanurate
[d] Reference (Polyester/Fiberglass)

Heat of Combustion and Efficiency

Values for ΔH_t, the net heat of complete combustion, were measured in an oxygen bomb calorimeter. Values of χ_{ch} and χ_c, the combustion efficiency and the convective fraction, were obtained by measuring the chemical and convective heat release rate, time integrating to obtain the total energy released and dividing by the total mass loss and ΔH_t. The radiative fraction of the combustion efficiency, χ_r, was assumed to be the difference between χ_{ch} and χ_c.

Effective Heat of Gasification

To account for the effects of char layer growth on the combustion characteristics, the following analytical formulation, based on modification of an analytical expression from Ref. 5, was used:

$$\dot{Q}''_{ch}\left[(t-t_p)/t_p\right]^{1/2} = (\Delta H_{ch}/L_e)\dot{q}''_n \qquad (5)$$

where t = time (s); $\dot{Q}''_{ch}$ = chemical heat release rate per unit surface area at time t (kW/m^2); t_p = time to peak heat release rate (s); L_e = "effective" heat of gasification (kJ/g); and $\dot{q}''_n$ = net heat flux assumed to be the difference between $\dot{q}''_e$ and $\dot{q}''_{cr}$ (kW/m^2). Figure 3 shows a plot of the left-hand side of Eq (5) versus the nondimensional time ratio $[(t-t_p)/t_p]^{1/2}$ for Samples 1, 5 and 6. The data in the figure indicate that Eq (5) is a reasonable representation within ± 5% for these char-forming materials. All L_e values reported in Table I are based on this procedure.

Vertical Flame Spread

"Apparent" upward flame spread velocities were determined from the heat release rate profiles for the 610 mm high samples in the 500 kW-Scale Apparatus. Each material exhibited an initial flash to the top of the sample

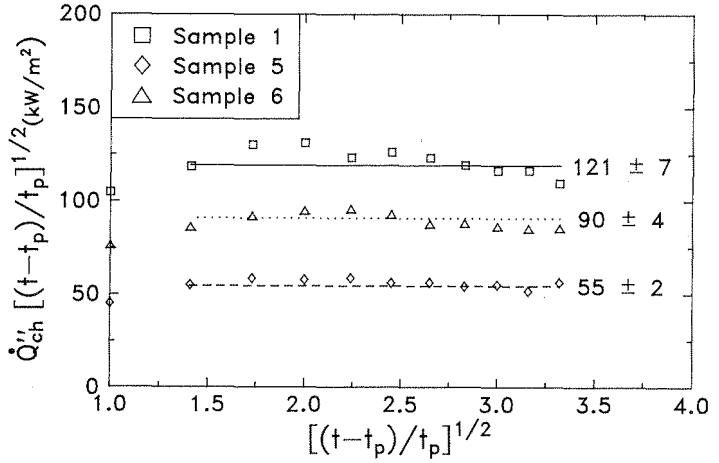

FIGURE 3. Flammability characterization versus nondimensional time.

followed by a rapid flame extinction to near the external flux zone (see Fig. 1). (This phenomenon was observed in all experimental scales). Peak heat release rates were observed to coincide with full involvement of the sample (i.e., flames flashing over the entire vertical surface). A height of 610 mm was therefore assigned to this peak value, with proportional values of height determined for each intermediate measured heat release rate. Subsequent differentiation of the calculated height versus time was used to determine an apparent flame spread velocity (v) [1], i.e.,

$$v = \frac{dh}{dt} = \frac{h_t}{E_t}\left(\frac{dE_i}{dt}\right) \qquad (6)$$

where h_t is the total height of the sample (mm); E_t is the total time-integrated energy released up to full involvement of the sample (kJ); and E_i is the instantaneous energy release (kJ). Figure 4, for example, shows v plotted versus h for Sample 1. The curve through the data in the figure is a second order polynomial fit, with the dashed lines indicating the value of

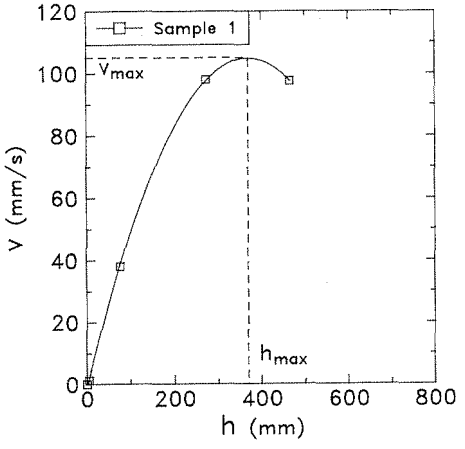

FIGURE 4. Flame spread velocity versus height.

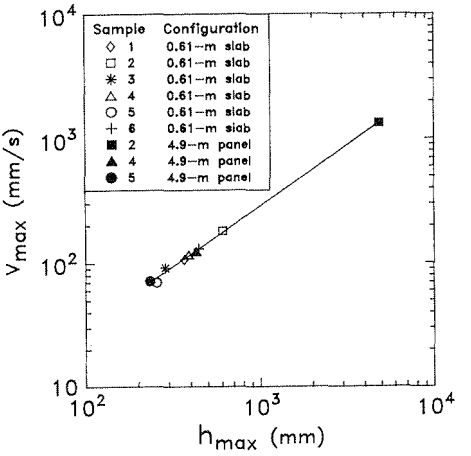

FIGURE 5. Maximum flame spread velocity versus height.

the maximum velocity, v_{max}, and its location, h_{max}. These two quantities were obtained by solution of the differentiated polynomial expression at zero acceleration (i.e., zero slope). The values of v_{max} and h_{max} derived in this fashion are listed in Table I. This technique was also used for the calculation of v_{max} and h_{max} for Samples 2, 4 and 5 selected for the 10,000 kW-Scale Apparatus experiments. All the data for v_{max} and h_{max} from both sets of experiments are plotted in Fig. 5. The data are well-fit by a linear curve of slope 0.30. The three sample materials tested in both scales exhibit some interesting characteristics. For the two isocyanurate samples (4 and 5), v_{max} (and the corresponding h_{max}) was virtually identical in the two scales (within ± 5%). However, the maximum velocities for Sample 2 were dramatically different (1320 versus 179 mm/s). This result was not unexpected since Sample 2 was the only material of the six tested in the 500 kW-Scale Apparatus where v_{max} occurred at the very top of the vertical slab (h_{max} = 610 mm). Also, in the 10,000 kW-Scale Apparatus, v_{max} occurred at the top of the panel (h_{max} = 4.9 m). Thus out of the six samples examined, only Sample 2 appears to have self-sustained propagation. For the other samples, v_{max} always resulted at a height less than the length of the sample, indicating flame front deacceleration and limited fire spread.

ANALYSIS

Extent of Fire Propagation

The extent of fire propagation in the 7.6-m Corner was determined by the visual damage at the conclusion of each experiment as shown in Figs. 6 and 7. The extent of propagation was also assessed by assuming the critical heat flux boundary defines the limit of propagation during the 15 min tests. Figure 6 shows the 14 kW/m^2 and Fig. 7 the 27 kW/m^2 critical heat flux boundary for Samples 2 and 4, respectively, superimposed on the visual damage boundary. An excellent agreement can be noted between the two types of assessments. It is also important to note that, in this panel configuration with inert metal facings, even Sample 2 (which indicated self-sustained flame spread behavior for the unfaced material) had limited extent of propagation.

An important unanswered question is how the critical heat flux boundary is reached in the Corner experiment and its relationship to the extent of

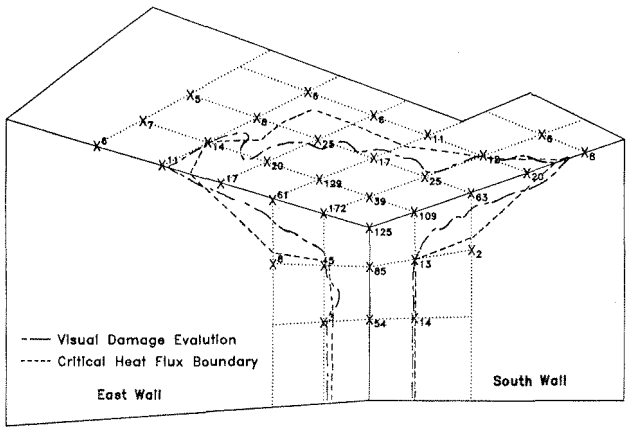

FIGURE 6. 7.6-m Corner heat flux distribution for Sample 2; x: calculated heat flux (kW/m^2).

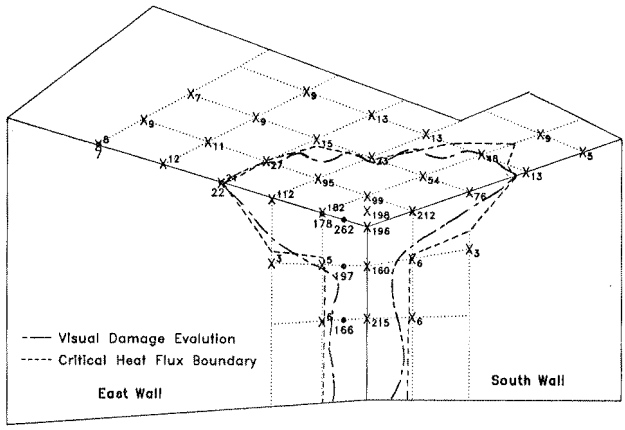

FIGURE 7. 7.6-m Corner heat flux distribution for Sample 4; •: measured heat flux (kW/m^2); x: calculated heat flux (kW/m^2).

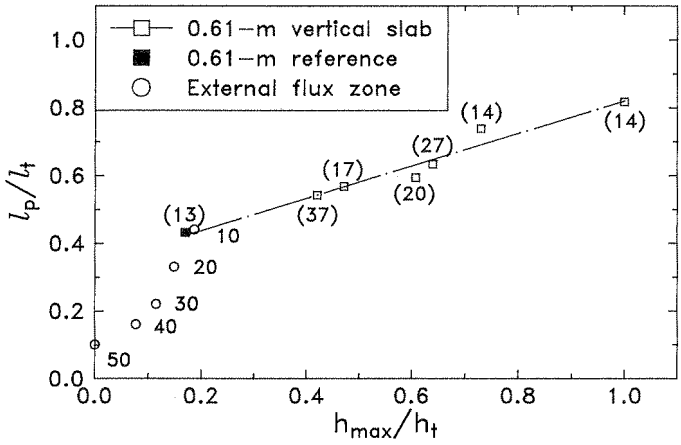

FIGURE 8. Extent of fire propagation in corner test versus relative location of maximum flame propagation velocity in small-scale. Numbers without parentheses are external heat flux values (kW/m^2); numbers with parentheses are critical heat fluxes (kW/m^2).

fire propagation in the 610 mm vertical sheet. Figure 8 shows ℓ_p/ℓ_t plotted against h_{max}/h_t; where ℓ_p is the average propagation length along the ceiling eaves of the East and South walls, ℓ_t is the total length available for propagation (11.6 m) in the 7.6-m Corner and h_t is the total length (610 mm) available in the 500 kW-scale experiment. The open circles followed by numbers are the heat fluxes from the ignition source in the 7.6-m Corner (Fig. 2) and from the 50 kW/m^2 external source in the 500 kW-Scale Apparatus (Fig. 1) given at comparable locations. The numbers given parenthetically are the critical heat flux values for the samples. The reference material, which had a very low heat release rate, contributed negligibly

small flame heat flux to the surface. The extent of fire propagation for the reference material was limited to the external heat flux location corresponding to its critical heat flux in both sets of experiments. While the extent of propagation in both scales of experiments was generally smaller for samples with higher critical flux values, the exceptions noted on the figure suggest that other factors are also important.

"Apparent" Velocity of Propagation

Previous work for upward flame propagation over polymers in cylindrical configurations [1] suggests that the flame propagation velocity is a function of the ratio of a heat release rate (e.g., Eq (3) to the surface thermal response (e.g., Eq (2)). Therefore, the following expression was used for correlation:

$$v = f\{[(\Delta H_i/L_e)/TRP](\dot{q}''_e+\dot{q}''_f-\dot{q}''_{cr})\} \quad (7)$$

where ΔH_i is the heat of combustion (i = chemical, radiative or convective) (kJ/g). Using the integration of the external heat flux versus height profile from Fig. 1, $\dot{q}''_e$ at h_{max} is 10 ± 3 kW/m^2. The average flame radiant heat flux was approximated [6] as 9.62 $\chi_r \dot{Q}'^{1/3}_{ch}$, or 20 ± 4 kW/m^2; while the convective heat flux was assumed constant [6] at 20 kW/m^2. From these estimated values and the data for v_{max}, ΔH_i, L_e, TRP and $\dot{q}''_{cr}$ from Table I, the relationship suggested by Eq (7) can be examined as shown in Fig. 9 with each sample indicated by its corresponding number. It can be noted that the best correlation is obtained using the convective heat of combustion, ΔH_c, where

$$v_{max} = 190\{([\Delta H_c/L_e]/TRP)(50-\dot{q}''_{cr})\}^{0.5}. \quad (8)$$

The implications of this relation are being explored further in our laboratory.

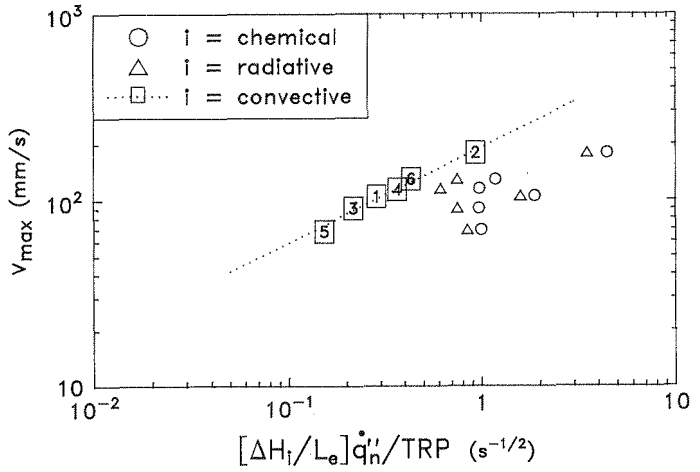

FIGURE 9. Relationship between maximum flame spread velocity and material flammability characteristics Framed numbers refer to sample designations given in Table 1.

SUMMARY

The fire spread behavior for char-forming insulating materials is not typical of noncharring materials. Upon ignition, a rapid surface flame spread is followed immediately by char layer formation and flame extinction, with the extent of fire propagation defined by the critical heat flux boundary. In wall/ceiling applications, metal facings limit the extent of fire spread even for materials exhibiting self-sustained fire propagation behavior. This may be an important consideration for wall fire models.

Reduced-scale propagation experiments are shown to properly delineate large scale behavior as well as indicate accelerative/deaccelerative flame spread velocities. The data suggest that the ratio of the convective heat release rate to the surface thermal response is important in vertical flame spread over char-forming insulations. This result is unexpected and is being further investigated.

ACKNOWLEDGMENTS

Contributions by Mr. M.M. Khan, for assistance in data analysis, Mr. E.R. Dunn and Mr. W.F. Maroni, for valuable information and insight, and Mr. S.D. Ogden, for assistance in data acquisition, are gratefully appreciated.

REFERENCES

1. Tewarson, A. and Khan, M.M., Twenty-Second Symposium (International) on Combustion, p. 1231, The Combustion Institute, 1988.

2. Newman, J.S., "Analysis of the FMRC Building Corner Test," Factory Mutual Research Corporation, Norwood, MA, FMRC J.I. 0Q5E5.RC, April 1989.

3. Newman, J.S., "Cost-Effective Method for Flammability Characterization of Alternative Polyols and Blowing Agents," in CFCs & the Polyurethanes Industry: Volume 2, ed. by F.W. Lichtenberg, Technomic Publishing Co., Lancaster, PA, 1989, p. 97.

4. Tewarson, A., Lee, J.L. and Pion, R.F., Eighteenth Symposium (International) on Combustion, p. 563, The Combustion Institute, 1981.

5. Delichatsios, M.A. and de Ris, J., "An Analytical Model for the Pyrolysis of Charring Materials," paper presented at Conseil International du Batiment meeting, Stockholm, Sweden, May 1983.

6. Delichatsios, M.A., "An Outline for a Comprehensive Model for the Burning and Upward Flame Spread on Charring Materials in Wall Fires," Factory Mutual Research Corporation, Norwood, MA, FMRC J.I. 0Q0J1.BU, August, 1988.